Published in final edited form as:
Stem Cells. 2010 July ; 28(7): 1260–1269. doi:10.1002/stem.455.

Dicer Ablation Impairs Prostate Stem Cell Activity and Causes Prostate Atrophy

Li Zhang[a], **Boyu Zhang**[a], **Joseph M. Valdez**[a], **Fen Wang**[b], **Michael Ittmann**[a], and **Li Xin**[a]
[a]Department of Molecular and Cellular Biology, Baylor College of Medicine, Houston, TX 77030 USA

[b]Texas A&M Health Science Center, Houston, TX 77030 USA

Abstract

Dicer is an RNase III enzyme essential for microRNA maturation. Dicer ablation in diverse tissues has been shown to block tissue differentiation, induce cell apoptosis, impair specialized cellular function, and perturb organ structures. To gain insight into the role of microRNAs in prostate tissue function and homeostasis, we conditionally disrupted Dicer activity in the mouse prostate using an ARR2PB-Cre. We demonstrated that Dicer activity is disrupted in both prostatic basal/stem cells and differentiated luminal cells. Dicer knockout murine prostates are smaller in size and mass and develop epithelial hypotrophy in ventral prostates by 4 months. Dicer ablation induces increased apoptosis in the prostate, predominantly in the differentiated luminal cells. Paradoxically, a concurrent increase in proliferation is observed in both basal/stem cells and luminal cells, presumably due to compensatory growth of the cells devoid of homologous recombination in response to the elevated cellular apoptosis. We have previously shown that Lin(CD31CD45Ter119)$^{-}$Sca-1^{+}CD49f^{high} (LSC) cells enrich for prostate stem cell activity. Through proliferation and differentiation, some LSC cells are capable of forming prostate spheres composed of cells at various stages of differentiation. Although LSC cells were expanded by threefold in *Dicer* knockout mice, the sphere-forming units of *Dicer* knockout prostate cells decreased by more than half compared with wild-type cells. In addition, most prostate spheres in the *Dicer* knockout culture were derived from cells that did not undergo homologous recombination. Our results demonstrate a critical role of microRNAs for the proliferative capacity of prostate stem cells and the maintenance of prostate homeostasis.

Keywords

Dicer; MicroRNAs; Prostate stem cells; Prostate spheres

Correspondence: Li Xin, Ph.D., Baylor College of Medicine, One Baylor Plaza, Houston, Texas 77030, USA. Telephone: 713-798-1650, Fax: 713-798-3017; xin@bcm.tmc.edu.

Author contribution: L. Z.: Conception and design, collection and/or assembly of data, data analysis and interpretation; B. Z.: collection and/or assembly of data, data analysis and interpretation; J. M V.: manuscript writing; F. W.: Provision of study material; M. I.: data analysis and interpretation; L. X.: Conception and design, manuscript writing, collection and/or assembly of data, data analysis and interpretation, final approval of manuscript.

Disclosure of Potential Conflicts of Interest
The authors indicate no potential conflicts of interest.

INTRODUCTION

miRNAs are a class of small single-stranded RNAs that play important roles in regulating developmental processes by generally repressing gene expression [1–3]. MicroRNAs are transcribed as long primary transcripts (pri-miRNAs), which are subsequently processed by a nuclear multiprotein Drosha-DGCR8 (Pasha) microprocessor complex and a cytoplamic RNase III enzyme Dicer to generate 19–25 nt mature miRNAs [3]. Although DGCR8 is required for the processing of the majority of microRNAs, Dicer is essential for the maturation of all microRNAs as well as some other endogenous small RNA species [4].

Gene knockout of *DGCR8* and *Dicer* results in global ablation of mature miRNAs [5,6]. Cell biological studies demonstrated that *DGCR8* and *Dicer* null embryonic stem cells are resistant to signaling inducing differentiation [6,7]. Conditional knockout of *DGCR8* and *Dicer* in diverse murine tissues also highlights the critical roles of miRNAs in organ morphogenesis [5,8–19], immune surveillance [20], angiogenesis [21], and fertility [22,23]. Common phenotypes observed in those studies are defects in tissue morphogenesis and function and an increase in cellular apoptosis. Of note, in most of these studies, Dicer activity is disrupted in specific cell types from the embryonic stage or immediately upon their specification at the adulthood. Hence, the resulting biology is a combined effect of *Dicer* ablation on tissue development and homeostasis.

So far, no study has been reported to investigate biological consequences of *Dicer* ablation in the prostate. There are three epithelial cell types in the prostate: the secretory luminal cell, basal cell, and a very rare neuroendocrine cell [24]. We previously showed that prostate stem cells reside in the basal cells and display a surface antigen expression profile of Lin(CD31, CD45, Ter-119)$^{-}$ Sca-1^{+}CD49f^{high} [25,26]. A bipotent self-renewing cell population that displays a luminal phenotype was also identified recently [27]. Using a low-density Taqman miRNA array, we showed that miRNAs are extensively expressed in the prostate [28]. Some miRNAs, such as the miR-200 family, are differentially expressed in the basal/stem cells and the differentiated luminal cells, suggesting that they may mediate signaling regulating cell self-renewal and differentiation [28].

In this study, we created a conditional mouse model to ablate *Dicer* in the prostate by using an *ARR2PB* Cre. *ARR2PB* is a composite rat probasin promoter [29]. Cre recombinase is expressed in the prostate, seminal vesicles, and ductus deferens at approximately 2–3 weeks postnatal when the *ARR2PB* composite promoter is activated by the androgen receptor [30]. By that time, prostate cell lineage commitment and glandular branching morphogenesis have largely been established. Previous studies showed that the probasin promoter is not only active in the luminal cells but also in the basal/stem cells [31]. The spatiotemporal expression pattern of this promoter avoids interference of prostate development by loss of Dicer activity and enables us to evaluate the role of miRNAs in the maintenance of prostate tissue and the responses of different prostate cell lineages toward Dicer ablation.

MATERIALS AND METHODS

Mouse Strains

The wild-type C57BL/6 and *Dicer1*^{tm1bdh}/J were purchased from the Jackson Laboratory (Bar Harbor, ME). The *ARR2PB-Cre* transgenic mice were from Dr. Fen Wang at the Institute of Bioscience and Technology, Texas A&M Health Science Center. All of the mice were housed and bred under the regulation of The Center for Comparative Medicine at the Baylor College of Medicine.

Regular and Real-Time PCR to Genotype and to Verify and Quantify *Dicer* Deletion

Genomic DNA was isolated from murine prostate cells using the DNeasy blood and tissue Kit (Qiagen, Valencia, CA). For single sphere PCR, single spheres were microscopically picked up and boiled in 100 μl DNase and RNase-free water for 5 minutes. Five microliter DNA solution was used as a template in a 20 μl PCR system. Polymerase chain reaction (PCR) analyses were performed to genotype and to determine whether the floxed Dicer alleles are excised. The primers are as below: *Dicer* forward: 5′ CCTGACAGTGACGGTC CAAAG 3′, *Dicer* reverse: 5′ CATGACTCTTCAACTCAAACT 3′, *Dicer* Del: 5′ CCTGAGCAAGGCAAGTCATTC 3′, R26 forward: 5′ CGAGGCGGATCACAAGCAATA 3′ and R26 reverse 5′ CTCTGCTGCCTCCTGGCTTCT 3′. Primers for real-time PCR to quantify cells that underwent homologous recombination in Dicer cKO mouse prostates are as follows: exon 24 forward, 5′ TCCAGGGGTCTTGACTGACT 3′; exon 24 reverse, 5′ CCAATGATGCAAAGATGGTG 3′; exon 21 forward, 5′ GAACATGCTGCACATCAAGG 3′; exon 21 reverse, 5′ GCAACCTTTTGCAGTTCACA 3′.

RNA Isolation and Quantitative RT-PCR

Total RNA was isolated from cells using the mir*V*ana miRNA isolation kit (Ambion, Austin, TX, http://www.ambion.com). Reverse transcription was performed using the Taqman micro-RNA RT kit (Applied Biosystems Incorporation, Foster City, CA). Quantitative RT-PCR was performed using the Taqman Power Sybrgreen master mix (Applied Biosystems) on a StepOne plus Real-Time PCR system (Applied Biosystems).

Fluorescence Activated Cell Sorting

Dissociated murine prostate cells were suspended in DMEM/10% FBS and stained with antibodies for 15 minutes at 4°C. The antibodies used were FITC-anti CD31, CD45, and Ter119 antibodies (eBioscience, San Diego, CA), PE-anti Sca-1 antibody (eBioscience), and Alexa 647-anti CD49f antibody (Biolegend, San Diego, CA, http://www.biolegend.com). Fluorescence activated cell sorting (FACS) analyses and sorting were performed by using the BD LSR II and Aria II, respectively (BD Biosciences, San Jose, CA, http://www.bdbiosciences.com).

Lentivirus Generation and Infection

The cDNA for a codon-optimized Cre recombinase (iCre) was cloned at the *XbaI* site of an FU-CRW vector [32], generating the FU-Cre-CRW vector. In this vector, iCre is driven by a human *Ubiquitin* promoter and is followed by a CMV promoter driving the expression of monomeric red fluorescent protein. Lentivirus preparation, titering, and infection of dissociated prostate cells were performed as described previously [33].

Prostate Sphere Assay

Prostate sphere assays were performed as previously described [34]. Dissociated prostate epithelial cells were prepared from 7- to 12-week-old C57BL/6, *Dicer*$^{fl/fl}$ and *ARR2PB-Cre;Dicer*$^{fl/fl}$ adult mice as described previously. In the prostate sphere assay, 1–5 × 10^4 dissociated prostate cells were cultured in 1:1 Matrigel/PrEGM [Matrigel (BD Biosciences, Two Oak Park, Bedford, MA)/PrEGM (Lonza, Walkersville, MD, http://www.lonza.com)].

Histology and Immunohistochemical Analyses

Histological and immunohistochemical analysis (IHC) analyses were performed as described previously [33]. Slides were made from formalin-fixed and paraffin-embedded (FFPE) prostate sphere cells or from frozen regenerated tissues. Tissue sections were either stained with H&E or the following antibodies: rabbit anti-AR (Santa Cruz Biotechnology

Inc., Santa Cruz, CA, http://www.scbt.com), mouse anti-p63 (4A4, Santa Cruz Biotechnology Inc.), mouse anti-cytokeratin 8 (clone 1E8; Covance, Berkeley, CA), rabbit anti-cytokeratin 5 (Covance), mouse anti-Chromagranin A (Chemicon, Temecula, MA, http://www.chemicon.com), rabbit anti-synaptophysin (Zymed, South San Francisco, CA), rabbit anti-Ki67 (Novocastro Laboratories Ltd., U.K.), rabbit anti-cleaved caspase three (Cell Signaling Technologies, Danvers, MA), and Deadend Fluometric terminal d-UTP end-labeling (TUNEL) system (Promega, Madison, WI, http://www.promega.-com). Biotinylated goat-anti-rabbit or rabbit-anti-mouse secondary antibodies and Strepavidin-conjugated horseradish peroxidase (Vector Laboratories, Burlingame, CA, http://www.vectorlabs.-com) was used for chromatic visualization. For fluorescence visualization, sections were stained with an Alexa Fluor 594 goat anti-rabbit IgG (H+L), Alexa Fluor 594 goat anti-mouse IgG (H+L) (Invitrogen, Carlsbad, CA, http://www.invitrogen.com) secondary antibody or Biotinylated goat-anti-rabbit or rabbit-anti-mouse secondary antibodies followed by Strepavidin-conjugated Alexa Fluor 488 or 595 (Invitrogen). Sections were counter-stained with DAPI in mounting medium (Vector Laboratories) and analyzed by fluorescent microscopy.

RESULTS

Dicer Ablation Results in Smaller Prostate Size and Mass

To investigate the overall function of microRNAs in the prostate, we crossed mice conditional for *Dicer* (*Dicer*$^{flox/flox}$) [5] with animals expressing an *ARR2PB-Cre* [30] (hereafter referred to as *PB-Cre*). *PB-Cre*;*Dicer*$^{flox/flox}$ mice (hereafter referred to as cKO mice) were generated at an expected mendelian ratio. Both cKO males and females exhibited normal weights and weaning behaviors as compared with littermate *PB-Cre*;*Dicer*$^{flox/wt}$ and *PB-Cre*$^{-}$;*Dicer*$^{flox/flox}$ controls (hereafter referred to as Het and WT controls, respectively) (data not shown).

Male urogenital systems including prostate, seminal vesicles, bladder, and urethra were collected from 2-month-old animals. Figure 1A shows representative images of the urogenital systems from WT, *Dicer* Het, and cKO mice. *Dicer* cKO and Het urogenital organs were significantly smaller and exhibited a reduction in mass, as compared with *Dicer* WT controls (Fig. 1B, mean urogenital organ mass at 2 months is 401.7 ± 31.7 mg for WT controls, 337.1 ± 38.7 mg for Het and 278.8 ± 37.5 mg for cKO animals, $n = 7$ for cKO and WT, $n = 12$ for Het; Student's t test was performed, $p = .0014$ between WT and cKO, $p = .0096$ between WT and Het, $p = .073$ between Het and cKO). Prostates were further separated from other urogenital tissues. Figure 1A shows anterior prostate lobes from WT, Het, and cKO mice. *Dicer* cKO prostates were also smaller and weighed less as compared with Het and WT prostates (Fig. 1C, mean prostate mass at P60 is 72.1 ± 6.32 mg for WT controls, 71.6 ± 9.34 mg for Het and 47.2 ± 4.60 mg for cKO animals, $n = 4$; $p = .0044$ between WT and cKO, $p = .0090$ between Het and cKO). However, no significant changes in ductal tip number in anterior prostates were noted, suggesting that prostate morphogenesis is not affected (data not shown). Prostates were dissociated into single cells through mechanical force and enzymatic digestion as was described previously [33]. Significantly less cells were obtained from *Dicer* cKO prostates as compared with the Het and WT controls (Fig. 1D, mean cell number per prostate at 2 months is 906,400 ± 68,981 for WT controls, 872,200 ± 173,322 for Het and 534,020 ± 38,198 for cKO animals, $n = 5$ for WT and cKO, whereas $n = 3$ for Het; $p = 5.6$ e-06 between WT and cKO, $p = .0045$ between Het and cKO).

Disrupting Dicer Activity Results in a Reduction of miRNA Expression in the Prostate

Expression of Cre recombinase starts at approximately 2–3 weeks postnatal when the *Probasin* promoter is activated in response to androgen stimulation. Recombination of the floxed *Dicer* allele was confirmed by PCR analysis of DNA extracted from 2-month-old mouse prostate tissues. As shown in Figure 2A, the WT and floxed *Dicer* alleles generated a 350 bp and a 420 bp product, respectively, using the *Dicer* forward and *Dicer* reverse primer set. Although the *Dicer* forward and *Dicer* Del primer set distinguishes the WT allele (1,300 bp), floxed allele (a band more than 2 kb) and the deletion allele (600 bp). The Cre-LoxP mediated homologous recombination disrupts Dicer enzymatic activity through deletion of 90 amino acids in its second RNase III domain [5], hence the mutant Dicer protein is indistinguishable from the wild-type Dicer by IHC and Western Blot analyses using currently available antibodies against Dicer. To further confirm that Dicer activity was disrupted, we measured the expression levels of eight prostate-expressing microRNAs in cKO, Het, and WT mouse prostates by Taqman miRNA analysis. Figure 2B shows that expression of most microRNAs in the Het mice were comparable with those in the WT mice. However, expression levels of all the tested microRNAs were reduced by 35%–75% in the cKO mice. The remaining microRNA expression is probably from nonepithelial cells in the prostate (stromal cells, blood cells, endothelial cells, etc.) and from epithelial cells that did not undergo homologous recombination.

Dicer Ablation Takes Place in Both Prostatic Basal/Stem and Luminal Cells

We previously demonstrated that prostate stem cells reside in basal cells and that different prostate cell lineages can be fractionated by FACS based on their surface antigen expression profiles [25,26]. Prostate basal/stem cells, luminal epithelial cells, and stromal cells are Lin(CD45CD31-Ter119)$^{-}$Sca-1^{+}CD49f^{high}, Lin^{-}Sca-1^{-}CD49f^{low}, Lin^{-}Sca-1^{+}CD49f^{-}, respectively. Previous studies have shown that the *Probasin* promoter is not only active in the luminal cells but also in the basal/stem cells [31]. To quantify the percentage of the cells that have undergone homologous recombination in individual cKO prostate cell lineages, we used a real-time PCR-based methodology. Two pairs of primers were designed to generate a 79 bp and a 62 bp amplicon from exon21 and exon24 of Dicer, respectively. On homologous recombination, exon24 will be removed from the genome, whereas exon21 is left intact. Hence, the ratio of the amount of exon24 and exon21 is representative of the percentage of the cells that did not undergo homologous recombination. Lineage markers, Sca-1 and CD49f, were used to FACS sort basal/stem cells, luminal cells, and stromal cells from 2-month-old *Dicer* cKO mice ($n = 5$). Genomic DNA from each cell fraction was extracted and real-time PCR was performed. DNA from *Dicer*$^{fl/fl}$ mice was used as a control, with its ratio of exon24/exon21 defined as 1. Figure 3 shows that less than 30% of basal/stem cells and luminal cells retained exon24, suggesting efficient *Dicer* deletion in both basal/stem cells and luminal cells. In contrast, more than 90% of stromal cells retained exon24, in agreement with previous knowledge that probasin is only expressed in epithelial cells.

Dicer Conditional Knockout Prostate Tissues Display Epithelial Atrophy

Histological analysis of the prostates from 2-month-old WT and cKO males showed no obvious differences (data not shown). *Dicer* cKO prostate glands are composed of one or two layers of epithelial cells surrounding lumen filled with eosinophilic secretions, suggesting that normal secretory function is maintained in cKO prostates. However, by 4 months, distinctive histologic changes were noted in cKO mouse prostates as compared with the WT controls (Fig. 4). Nests of cells with darker hematoxylin staining were observed in dorsolateral lobes of cKO prostates. Compared with the columnar shape of the cells in the WT ventral prostate lobes, cells in the cKO ventral lobes were extremely thin, characteristic of epithelial hypotrophy. Occasionally, a transition of cell shape from flat to cuboidal (Fig. 4, blue arrow) was seen in individual glands, indicating mosaic homologous recombination

in prostate epithelial cells. The lobe-specific phenotypic variation has been reported in several other transgenic models that used the probasin promoter [35–37]. Using the quantitative PCR assay described in Figure 3, we did not detect a significantly higher efficiency of Cre-mediated homologous recombination in ventral prostate lobes, suggesting that this is not the reason for the more distinct hypotrophic phenotype in ventral prostate lobes (Supporting Information Fig. S1). Interestingly, we found that Dicer expression in the ventral lobes of wild-type mice is approximately 1.25-fold of that in other lobes (Supporting Information Fig. S1). This trivial intrinsic difference in gene expression profiles between individual prostate lobes may partially explain the phenotypic variations.

Dicer Ablation Induces an Expansion of Basal/Progenitor Cells

To further investigate potential biological consequences resulting from loss of function of Dicer, we evaluated the cell lineage composition in cKO mouse prostates. We measured the cell lineage composition in 2-month-old WT, Het, and cKO mouse prostates ($n = 4$ for WT and $n = 3$ for Het and cKO) by FACS as described previously. As shown in Figure 5A, 5B, we noticed a significant increase in basal/stem cell composition in the cKO and Het as compared with the WT controls (mean basal/stem cell percentage in 2-month-old prostates is 2.63% ± 0.68% for WT controls, 4.63% ± 0.21% for Het and 7.07% ± 0.46% for cKO animals; $p = .00020$ between WT and cKO, $p = .0047$ between Het and cKO). Compared with the WT mice, *Dicer* cKO mice, but not the Hets, display a significant decrease in luminal cell composition (mean luminal cell percentage is 62.22% ± 6.15% for WT controls, 63.30% ± 3.00% for Het and 49.83% ± 2.93% for cKO animals; $p = .025$ between WT and cKO). In contrast, stromal cell composition in Dicer cKO mice increased with a marginal statistical significance (mean stromal cell percentage is 19.48% ± 5.68% for WT controls, 14.97% ± 4.22% for Het and 29.70% ± 3.94% for cKO animals; $p = .046$ between WT and cKO).

In murine prostate, basal cells appear triangular in shape with very little cytoplasm. They usually form a punctuated cell layer between basement membrane and luminal cells. Consistent with the FACS data, we noticed a remarkable increase in K5 positive basal cell composition in cKO prostates by immunohistochemistry (Fig. 5C). Basal cells in cKO prostates packed tightly and formed a continuous layer surrounding luminal cells. P63 is another marker for basal cells. It is a transcription factor belonging to the P53 superfamily and has been shown to be critical for the maintenance and the proliferative potential of stem cells in several different organ systems [38,39]. Consistently, there is also a dramatic increase in the P63 positive cells in the cKO prostates compared with controls (Fig. 5D). Mean P63 positive cells in 100 cells in ventral prostates is 9.99 ± 3.71 for WT mice versus 29.00 ± 3.01 for cKO mice ($p = 4.88$ e-06) (Fig. 5E). Additionally, P63 positive cells in the cKO prostates displayed an enlarged nucleus as compared with those in the control prostates (Fig. 5D).

In contrast, there is no difference in the staining patterns of the luminal cell markers K8 (Fig. 5A) and the androgen receptor (data not shown) and the neuroendocrine cell markers synaptophysin and chromagranin A (data not shown) in cKO and WT prostates. These data demonstrate that there is a preferential expansion of basal/stem cells in the *Dicer* cKO prostates. It should be noted that besides active expansion of the $Lin(CD31CD45Ter119)^{-}Sca\text{-}1^{+}CD49f^{high}$ (LSC) population, decreased luminal cell composition also partially contributes to the increased percentage of the LSC cells in the cKO mice.

Increased Proliferation and Apoptosis in *Dicer* cKO Mouse Prostates

We sought to investigate whether deregulation of cell proliferation and apoptosis accounts for the reduction in organ size and mass as well as the changes in lineage composition in *Dicer* cKO mouse prostates. A significantly increased percentage of Ki67 positive proliferating cells were detected in 4-month-old cKO mouse prostates (Fig. 6Ai–Aiv, 0.75 ± 0.25 Ki67 positive cells per 100 cells in the control vs. 5.43 ± 1.52 Ki67 positive cells per 100 cells in *Dicer* cKO; $p = .00011$). Increased proliferation was also prominent in 2-month-old cKO prostates (data not shown). Proliferating cells were also observed in atrophic epithelia in the cKO ventral prostate (Fig. 6Aiii, arrows). A fraction of Ki67 positive cells (22.3% ± 11.3%) express the basal cell marker P63, whereas the remaining Ki67 positive cells did not. This suggests that both basal/stem cells and luminal cells underwent increased proliferation (Fig. 6Av). We also evaluated activation of caspase-3 and TUNEL in the prostate to determine cellular apoptosis. The wild-type prostate showed very rare events of apoptosis (data not shown), whereas cKO prostate displayed a significantly increased apoptotic index (Fig. 6Bi–Biii, 0.13 ± 0.22 cleaved caspase three positive cells per 100 cells in the control vs. 1.15 ± 0.55 cleaved caspase three positive cells per 100 cells in *Dicer* cKO; $p = .00021$). Most apoptotic cells were luminal cells because they did not express the basal cell marker P63 (Fig. 6Biv). These results demonstrate a concurrent cellular proliferation and apoptosis in *Dicer* cKO mouse prostates and implicate that differentiated luminal cells are more sensitive to Dicer ablation and tend to succumb to apoptosis in response to loss of microRNA biogenesis. The increased cell proliferation is probably due to the compensatory growth of the cells that did not undergo homologous recombination in response to elevated cellular apoptosis.

Dicer Ablation Impairs the Capacity of Prostate Stem Cells to Form Prostate Spheres In Vitro

We previously showed that when cultured inside matrigel in the presence of a defined serum free PREGM media, prostate stem cells are capable of forming clonal spheroids that can be serially passaged, demonstrating their capacity for self-renewal [34]. We sought to use this assay to investigate whether disrupting Dicer activity affects prostate stem cell activity. Dissociated single prostate cells were prepared from 7-week-old cKO animals and WT littermate controls. Cells were cultured in the prostate sphere assay. Prostate spheres grew out from both groups after a 7- to 10-day incubation. The sphere-forming unit (SFU) of the knockout cells was significantly lower compared with the control WT cells (Fig. 7A, 1.34% ± 0.28% for the WT cells vs. 0.54% ± 0.03% for the knockout cells; $p = 4.7$ e-08). The size of the prostate spheres in both groups ranged from 100 to 250 μm after a 7- to 10-day culture and the size distribution of the formed prostate spheres appeared similar in both groups (data not shown).

To investigate the genotype of the cellular origin of the formed prostate spheres, we picked up a total of 84 single prostate spheres from four independent *Dicer* cKO prostate sphere cultures and performed PCR analysis as described in *Materials and Methods* section. Genomic DNA from *Dicer* cKO and $Dicer^{fl/fl}$ mouse prostates were used as positive and negative controls, respectively. We were able to amplify a 330 bp fragment from the *Rosa26* locus of 72 spheres, demonstrating that genomic DNA qualities from these samples were good. However, the Dicer deletion band was only detected from 17 of 72 spheres, demonstrating that the majority of the outgrown spheres were derived from the basal/stem cells that did not undergo homologous recombination (Supporting Information Fig. S2). As the picked single spheres may be contaminated with *Dicer* cKO cells that did not form spheres yet remained alive in the culture, it is possible that some of those 17 spheres may still be derived from prostate stem cells that did not undergo homologous recombination.

Taqman miRNA assays were performed to evaluate the expression levels of seven prostate-expressing miRNAs in the prostate sphere cultures. Figure 7B shows that the expression of the tested miRNAs in the cKO culture was either unchanged or reduced by less than 40%. We showed in Figure 2B that the expressions of most tested miRNAs were reduced by more than 40% in cKO mice when total prostate cells were used for the Taqman assay. This further corroborates that cells devoid of homologous recombination were enriched in the prostate sphere culture. *Dicer* null spheres and *Dicer* null epithelial cells that did not form spheres but remained alive in the culture may account for the reduction of miRNA expression in the Dicer cKO prostate sphere culture. Overall, these results demonstrate that on *Dicer* ablation in spite of an expansion of cells phenotypic of prostatic basal/stem cells, those cells are less competent in forming prostate spheres in vitro.

To further corroborate directly that Dicer ablation impairs the capacity of the prostate stem cells to form spheres, we infected $Dicer^{fl/fl}$ prostate cells by lentivirus that expresses Cre recombinase and evaluated their capacity to form prostate spheres in vitro. We generated an FU-Cre-CRW vector that expresses Cre and RFP driven by human ubiquitin and CMV promoters, respectively. Cre expression does not impair prostate sphere forming activity (data not shown). Twenty-five thousand $Dicer^{fl/fl}$ prostate cells from 2-month-old mice were infected separately with the FU-Cre-CRW lentivirus and the empty FU-CRW virus that only expresses RFP at an M.O.I. of 20 and incubated in the prostate sphere assay. Prostate spheres formed in both groups after 7-day incubation. As not all cells were infected by the lentivirus, some spheres did not express RFP. We counted total spheres as well as red and nonred spheres. Figure 7C shows that the SFUs of the RFP group and the Cre group were approximately the same in the first generation of the prostate sphere culture. The percentages of red spheres were also comparable between the two groups (74% in the RFP group vs. 71% in the Cre group) (Fig. 7D). Genomic DNAs were extracted from both groups and the PCR assay described in Figure 2A was used and demonstrated that Dicer ablation only occurred in the Cre group (data not shown). Interestingly, when we passaged the prostate spheres and grew them for the second-generation, the SFU of the Cre group decreased significantly compared with the RFP group (2.10% in the RFP group vs. 1.07% in the Cre group, $p < .05$, Fig. 7C). In addition, the percentage of red spheres in the Cre group also dropped significantly after the passage (71% in the first generation vs. 38% in the second generation), whereas the percentage of red spheres decreased slightly in the RFP group (74% in the first generation vs. 62% in the second generation) (Fig. 7D). Overall, these data directly demonstrate that Dicer ablation impairs the capacity of basal/stem cells in forming prostate spheres in vitro. We probably did not observe any difference in sphere forming activity in the first-generation prostate sphere culture because micro-RNAs and Dicer expressed before Cre-mediated homologous recombination had a relatively long half-life and degraded only after prolonged culture.

DISCUSSION

Increased Proliferation Index in the *Dicer cKO* Mouse Prostate

Our study aims to investigate the role of microRNAs in the maintenance and the function of individual prostate cell lineages. Dicer activity has been specifically disrupted in more than a dozen tissue/cell types. The resulting biological consequences are quite versatile. Severe phenotypes include interference of tissue differentiation (the pancreatic beta cells and the B lymphoid cells) [13,40] and organ structure (skin and kidney) [8,9,14–16]. Milder phenotypes induced by Dicer ablation are tissue hypoplasia due to increased apoptosis (the skeletal muscle and neuron) [18,41] and deregulation of specialized cell functions (liver, testicles, ovary, and blood vessel) [21,23,42,43]. We found that Dicer ablation induces an elevated apoptotic index in the prostate and leads to epithelial hypotrophy.

A surprising observation in our study is an increased proliferation index in both the basal/stem cells and luminal cell lineages. A similar observation has been reported previously in a hepatocyte-specific Dicer knockout model, in which increased proliferation is accompanied by overwhelming apoptosis [44]. Because of technical limitation, we were not able to directly address whether this is a biological consequence resulting from *Dicer* ablation. This is unlikely to be true, as *Dicer* null cells are incompetent in proliferation in in vitro prostate sphere culture. In addition, we showed that *PB-Cre* mediated homologous recombination is not complete in prostate epithelia and 30% of cells in both the basal/stem cells and luminal cells still retain intact *Dicer* alleles. Therefore, the concurrent proliferation and apoptosis may reflect the incomplete penetrance of homologous recombination mediated gene ablation as well as the intrinsic capacity of the tissues for regeneration. It is more likely that cells devoid of homologous recombination undergo proliferation to compensate for tissue loss from apoptosis and try to restore normal tissue structures.

Differential Responses of Prostate Stem Cells and Luminal Cells Toward Loss of miRNA Biogenesis

Basal/stem cells and luminal cells in the *Dicer* cKO mice seem to tolerate *Dicer* ablation differentially for their survival. We showed in Figure 6 that most apoptotic cells in *Dicer* cKO mouse prostates were differentiated luminal cells and apoptotic basal cells were very rare. As a consequence, the percentage of luminal cells in *Dicer* cKO prostates decreased significantly. As homologous recombination took place at the same frequency in these two cell lineages (Fig. 3), we conclude that differentiated luminal cells are more sensitive to loss of miRNA biogenesis and tend to succumb to apoptosis. In contrast to the degeneration of differentiated luminal cells, there is an expansion of the cells that are phenotypic of the basal cells in *Dicer* cKO prostates, which is probably due to the combined effects of a sustained survival of *Dicer* null basal/stem cells and a compensatory proliferation of basal/stem cells with intact *Dicer*. These data suggest that basal/stem cells are more tolerant to loss-of-function of Dicer for their survival. Nevertheless, the proliferative capacities of the basal/stem cells are impaired, as they are incompetent to proliferate and differentiate to form prostate spheres in vitro.

A similar observation was reported in the neural system that differentiated neurons are more dependent on miRNA-mediated regulation than neural stem cells [18]. The molecular mechanisms underlying this differential cellular response toward loss of miRNA biogenesis have been gradually unveiled. MiRNAs usually repress gene expression at posttranscriptional levels through perfect or imperfect complementarity with mostly 3′UTR of mRNAs [45]. Alternative polyadenylation of mRNAs results in changes in 3′UTR length, hence affecting gene regulation by miRNAs [46]. Recently, it was shown that terminally differentiated cells mostly have mRNAs with full-length 3′UTRs. In contrast, immature stem/progenitor cells, proliferating cells, and transformed cells express mRNAs with shorter 3′UTRs [47–49]. This implies that gene regulation by miRNAs in stem, proliferating, and transformed cells is relatively less tense and they are therefore less sensitive to global ablation of microRNA biogenesis, which is consistent with our observation that basal/stem cells are less sensitive than differentiated luminal cells toward loss of miRNA biogenesis for their survival. However, microRNAs as fine regulators for gene expression become critical during cell differentiation when the precision and robustness of gene expression must be regulated tightly. In accordance, the potential of *Dicer* null prostate stem cells to proliferate and differentiate into prostate spheres is significantly impaired.

Supplementary Material

Refer to Web version on PubMed Central for supplementary material.

Acknowledgments

We thank Dr. Jeffrey Rosen for helpful discussions, the Cytometry and Cell Sorting Facility at the Baylor College of Medicine for technical support, Dr. Yi Li and lab members for technical help in immunohistochemical staining. L.X. was supported by NIH K99CA125937 and institutional funds from Baylor College of Medicine.

REFERENCES

1. Ambros V. The evolution of our thinking about microRNAs. Nat Med 2008;14:1036–1040. [PubMed: 18841144]
2. Ruvkun G. The perfect storm of tiny RNAs. Nat Med 2008;14:1041–1045. [PubMed: 18841145]
3. Stefani G, Slack FJ. Small non-coding RNAs in animal development. Nat Rev Mol Cell Biol 2008;9:219–230. [PubMed: 18270516]
4. Babiarz JE, Ruby JG, Wang Y, et al. Mouse ES cells express endogenous shRNAs, siRNAs, and other Microprocessor-independent, Dicer-dependent Small RNAs. Genes Dev 2008;22:2773–2785. [PubMed: 18923076]
5. Harfe BD, McManus MT, Mansfield JH, et al. The RNaseIII enzyme Dicer is required for morphogenesis but not patterning of the vertebrate limb. Proc Natl Acad Sci USA 2005;102:10898–10903. [PubMed: 16040801]
6. Wang Y, Medvid R, Melton C, et al. DGCR8 is essential for micro-RNA biogenesis and silencing of embryonic stem cell self-renewal. Nat Genet 2007;39:380–385. [PubMed: 17259983]
7. Kanellopoulou C, Muljo SA, Kung AL, et al. Dicer-deficient mouse embryonic stem cells are defective in differentiation and centromeric silencing. Genes Dev 2005;19:489–501. [PubMed: 15713842]
8. Yi R, O'Carroll D, Pasolli HA, et al. Morphogenesis in skin is governed by discrete sets of differentially expressed microRNAs. Nat Genet 2006;38:356–362. [PubMed: 16462742]
9. Andl T, Murchison EP, Liu F, et al. The miRNA-processing enzyme dicer is essential for the morphogenesis and maintenance of hair follicles. Curr Biol 2006;16:1041–1049. [PubMed: 16682203]
10. Mudhasani R, Zhu Z, Hutvagner G, et al. Loss of miRNA biogenesis induces p19Arf-p53 signaling and senescence in primary cells. J Cell Biol 2008;181:1055–1063. [PubMed: 18591425]
11. Soukup GA, Fritzsch B, Pierce ML, et al. Residual microRNA expression dictates the extent of inner ear development in conditional Dicer knockout mice. Dev Biol 2009;328:328–341. [PubMed: 19389351]
12. Harris KS, Zhang Z, McManus MT, et al. Dicer function is essential for lung epithelium morphogenesis. Proc Natl Acad Sci USA 2006;103:2208–2213. [PubMed: 16452165]
13. Lynn FC, Skewes-Cox P, Kosaka Y, et al. MicroRNA expression is required for pancreatic islet cell genesis in the mouse. Diabetes 2007;56:2938–2945. [PubMed: 17804764]
14. Shi S, Yu L, Chiu C, et al. Podocyte-selective deletion of dicer induces proteinuria and glomerulosclerosis. J Am Soc Nephrol 2008;19:2159–2169. [PubMed: 18776119]
15. Harvey SJ, Jarad G, Cunningham J, et al. Podocyte-specific deletion of dicer alters cytoskeletal dynamics and causes glomerular disease. J Am Soc Nephrol 2008;19:2150–2158. [PubMed: 18776121]
16. Ho J, Ng KH, Rosen S, et al. Podocyte-specific loss of functional microRNAs leads to rapid glomerular and tubular injury. J Am Soc Nephrol 2008;19:2069–2075. [PubMed: 18832437]
17. Pastorelli LM, Wells S, Fray M, et al. Genetic analyses reveal a requirement for Dicer1 in the mouse urogenital tract. Mamm Genome 2009;20:140–151. [PubMed: 19169742]
18. De Pietri Tonelli D, Pulvers JN, Haffner C, et al. miRNAs are essential for survival and differentiation of newborn neurons but not for expansion of neural progenitors during early neurogenesis in the mouse embryonic neocortex. Development 2008;135:3911–3921. [PubMed: 18997113]
19. Cuellar TL, Davis TH, Nelson PT, et al. Dicer loss in striatal neurons produces behavioral and neuroanatomical phenotypes in the absence of neurodegeneration. Proc Natl Acad Sci USA 2008;105:5614–5619. [PubMed: 18385371]

20. Liston A, Lu LF, O'Carroll D, et al. Dicer-dependent microRNA path-way safeguards regulatory T cell function. J Exp Med 2008;205:1993–2004. [PubMed: 18725526]
21. Suarez Y, Fernandez-Hernando C, Yu J, et al. Dicer-dependent endothelial microRNAs are necessary for postnatal angiogenesis. Proc Natl Acad Sci USA 2008;105:14082–14087. [PubMed: 18779589]
22. Otsuka M, Zheng M, Hayashi M, et al. Impaired microRNA processing causes corpus luteum insufficiency and infertility in mice. J Clin Invest 2008;118:1944–1954. [PubMed: 18398510]
23. Papaioannou MD, Pitetti JL, Ro S, et al. Sertoli cell Dicer is essential for spermatogenesis in mice. Dev Biol 2009;326:250–259. [PubMed: 19071104]
24. Abate-Shen C, Shen MM. Molecular genetics of prostate cancer. Genes Dev 2000;14:2410–2434. [PubMed: 11018010]
25. Lawson DA, Xin L, Lukacs RU, et al. Isolation and functional characterization of murine prostate stem cells. Proc Natl Acad Sci USA 2007;104:181–186. [PubMed: 17185413]
26. Xin L, Lawson DA, Witte ON. The Sca-1 cell surface marker enriches for a prostate-regenerating cell subpopulation that can initiate prostate tumorigenesis. Proc Natl Acad Sci USA 2005;102:6942–6947. [PubMed: 15860580]
27. Wang X, Kruithof-de Julio M, Economides KD, et al. A luminal epithelial stem cell that is a cell of origin for prostate cancer. Nature 2009;461:495–500. [PubMed: 19741607]
28. Zhang L, Zhao W, Valdez JM, et al. Low-density Taqman miRNA array reveals miRNAs differentially expressed in prostatic stem cells and luminal cells. Prostate 2009;70:297–304. [PubMed: 19827049]
29. Zhang J, Thomas TZ, Kasper S, et al. A small composite probasin promoter confers high levels of prostate-specific gene expression through regulation by androgens and glucocorticoids in vitro and in vivo. Endocrinology 2000;141:4698–4710. [PubMed: 11108285]
30. Jin C, McKeehan K, Wang F. Transgenic mouse with high Cre recombinase activity in all prostate lobes, seminal vesicle, and ductus deferens. Prostate 2003;57:160–164. [PubMed: 12949940]
31. Mulholland DJ, Xin L, Morim A, et al. Lin-Sca-1+CD49fhigh stem/progenitors are tumor-initiating cells in the Pten-null prostate cancer model. Cancer Res 2009;69:8555–8562. [PubMed: 19887604]
32. Xin L, Teitell MA, Lawson DA, et al. Progression of prostate cancer by synergy of AKT with genotropic and nongenotropic actions of the androgen receptor. Proc Natl Acad Sci USA 2006;103:7789–7794. [PubMed: 16682621]
33. Xin L, Ide H, Kim Y, et al. In vivo regeneration of murine prostate from dissociated cell populations of postnatal epithelia and urogenital sinus mesenchyme. Proc Natl Acad Sci USA 2003;100 Suppl 1:11896–11903. [PubMed: 12909713]
34. Xin L, Lukacs RU, Lawson DA, et al. Self-renewal and multilineage differentiation in vitro from murine prostate stem cells. Stem Cells 2007;25:2760–2769. [PubMed: 17641240]
35. Han G, Buchanan G, Ittmann M, et al. Mutation of the androgen receptor causes oncogenic transformation of the prostate. Proc Natl Acad Sci USA 2005;102:1151–1156. [PubMed: 15657128]
36. Stanbrough M, Leav I, Kwan PW, et al. Prostatic intraepithelial neoplasia in mice expressing an androgen receptor transgene in prostate epithelium. Proc Natl Acad Sci USA 2001;98:10823–10828. [PubMed: 11535819]
37. Bruxvoort KJ, Charbonneau HM, Giambernardi TA, et al. Inactivation of Apc in the mouse prostate causes prostate carcinoma. Cancer Res 2007;67:2490–2496. [PubMed: 17363566]
38. Signoretti S, Pires MM, Lindauer M, et al. p63 regulates commitment to the prostate cell lineage. Proc Natl Acad Sci USA 2005;102:11355–11360. [PubMed: 16051706]
39. Senoo M, Pinto F, Crum CP, et al. p63 Is Essential for the proliferative potential of stem cells in stratified epithelia. Cell 2007;129:523–536. [PubMed: 17482546]
40. Koralov SB, Muljo SA, Galler GR, et al. Dicer ablation affects anti-body diversity and cell survival in the B lymphocyte lineage. Cell 2008;132:860–874. [PubMed: 18329371]
41. O'Rourke JR, Georges SA, Seay HR, et al. Essential role for Dicer during skeletal muscle development. Dev Biol 2007;311:359–368. [PubMed: 17936265]

42. Nagaraja AK, Andreu-Vieyra C, Franco HL, et al. Deletion of Dicer in somatic cells of the female reproductive tract causes sterility. Mol Endocrinol 2008;22:2336–2352. [PubMed: 18687735]
43. Sekine S, Ogawa R, McManus MT, et al. Dicer is required for proper liver zonation. J Pathol 2009;219:365–372. [PubMed: 19718708]
44. Sekine S, Ogawa R, Ito R, et al. Disruption of Dicer1 induces dysregulated fetal gene expression and promotes hepatocarcinogenesis. Gastroenterology 2009;136:2304–2315. e1–e4. [PubMed: 19272382]
45. Bartel DP. MicroRNAs: Target recognition and regulatory functions. Cell 2009;136:215–233. [PubMed: 19167326]
46. Tian B, Hu J, Zhang H, et al. A large-scale analysis of mRNA polyadenylation of human and mouse genes. Nucleic Acids Res 2005;33:201–212. [PubMed: 15647503]
47. Ji Z, Lee JY, Pan Z, et al. Progressive lengthening of 3′ untranslated regions of mRNAs by alternative polyadenylation during mouse embryonic development. Proc Natl Acad Sci USA 2009;106:7028–7033. [PubMed: 19372383]
48. Sandberg R, Neilson JR, Sarma A, et al. Proliferating cells express mRNAs with shortened 3′ untranslated regions and fewer microRNA target sites. Science 2008;320:1643–1647. [PubMed: 18566288]
49. Mayr C, Bartel DP. Widespread shortening of 3′UTRs by alternative cleavage and polyadenylation activates oncogenes in cancer cells. Cell 2009;138:673–684. [PubMed: 19703394]

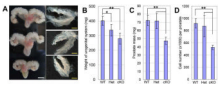

Figure 1.

Dicer ablation results in smaller prostate size and mass. **(A):** Representative images of urogenital systems and anterior prostate lobes from 2-month-old *Dicer* cKO, Het, and WT mice. White bars = 50 mm, yellow bars = 10 mm. **(B–D):** Bar graphs compare the weights of urogenital systems and total prostates and total cell number per prostate in 2-month-old *Dicer* cKO, Het, and WT mice. Error bars represent means and STD from 4 to 11 mice. *, $p < .001$; **, $p < .005$.

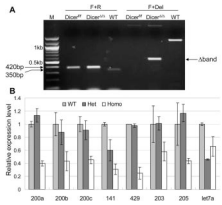

Figure 2.

Dicer ablation results in a reduction of miRNA expression in the prostate. **(A):** PCR analysis confirms the homologous recombination at the DNA level. **(B):** Expression of eight miRNAs in WT, Dicer Het, and cKO prostate by Taqman miRNA assays. SnoRNA234 was used as an internal control. Results were from two different animals in each group. Error bars represent means and STD. Statistical significant differences ($p < .05$) were observed between expression in the WT and KO prostate cells for miR-200a, miR-200c, miR-141, miR-429, and miR-205.

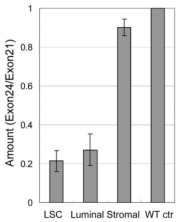

Figure 3.

Dicer ablation takes place in both prostatic basal/stem cells and luminal cells. The percentage of the cells that did not undergo homologous recombination was represented by expression level of exon24 versus that of exon21 (ratio Exon24/exon21) by Real-time PCR. Analysis was performed using pooled DNA from five mice. Error bars represent means and STD. Abbreviation: LSC, Lin(CD31CD45Ter119)$^{-}$ Sca-1^{+}CD49f^{high}.

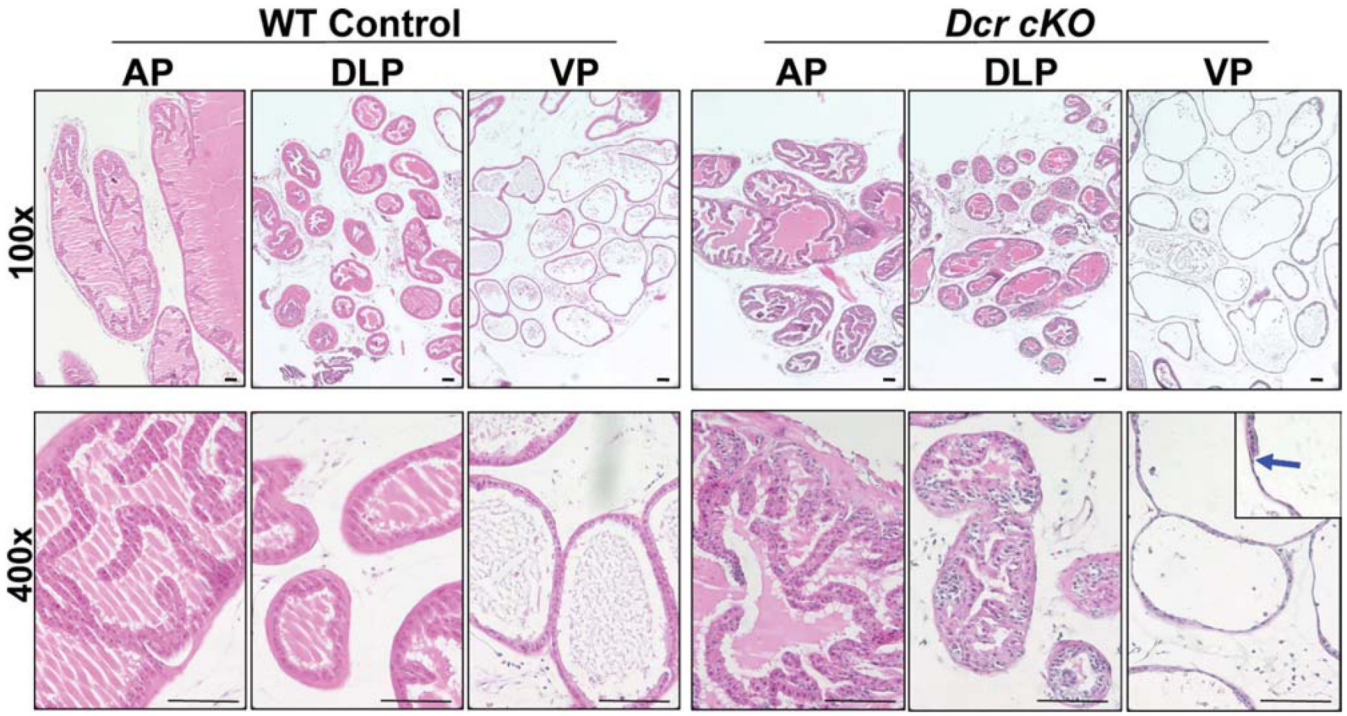

Figure 4.

Dicer cKO prostate tissues display epithelial hypotrophy. H&E staining of the WT and cKO prostate in low (upper panels, ×100) and high (lower panels, ×400) magnification. The blue arrow highlights a transition from normal to atrophic epithelial structure. Bars = 100 μm. Abbreviations: AP, anterior prostates; DLP, dorsolateral prostates; VP, ventral prostates.

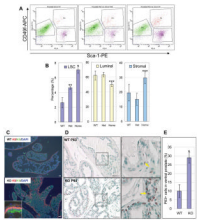

Figure 5.

Dicer ablation induces an expansion of basal/stem cells in the prostate. **(A):** Representative fluorescence-activated cell sorting plots analyzing cell lineage composition in 2-month-old *Dicer* cKO, Het, and WT prostates. Basal/stem cells, luminal cells, and stromal cells are Lin(CD45CD31Ter119)$^{-}$Sca-1^{+}CD49f^{high}, Lin^{-}Sca-1^{-}CD49f^{low}, Lin^{-}Sca-1^{+}CD49f^{-}, respectively. **(B):** Bar graphs summarize the percentages of basal/stem cells, luminal cells, and stromal cells. Error bars represent means and STD from 3 to 4 mice. *, $p < .0005$; **, $p < .005$; ***, $p < .05$. **(C,D):** IHC analyses of basal/stem cell markers keratin5 (K5) and P63 and luminal cell marker keratin8 (K8). Yellow arrows point to P63 positive cells. Bars = 100 μm. **(E):** Bar graph shows the percentage of P63 positive cells in ventral prostates of 2-month-old mice. Abbreviations: DAPI, 40′,6-diamidino-2-phenylindole; LSC, Lin(CD31CD45Ter119)$^{-}$Sca-1^{+}CD49f^{high}.

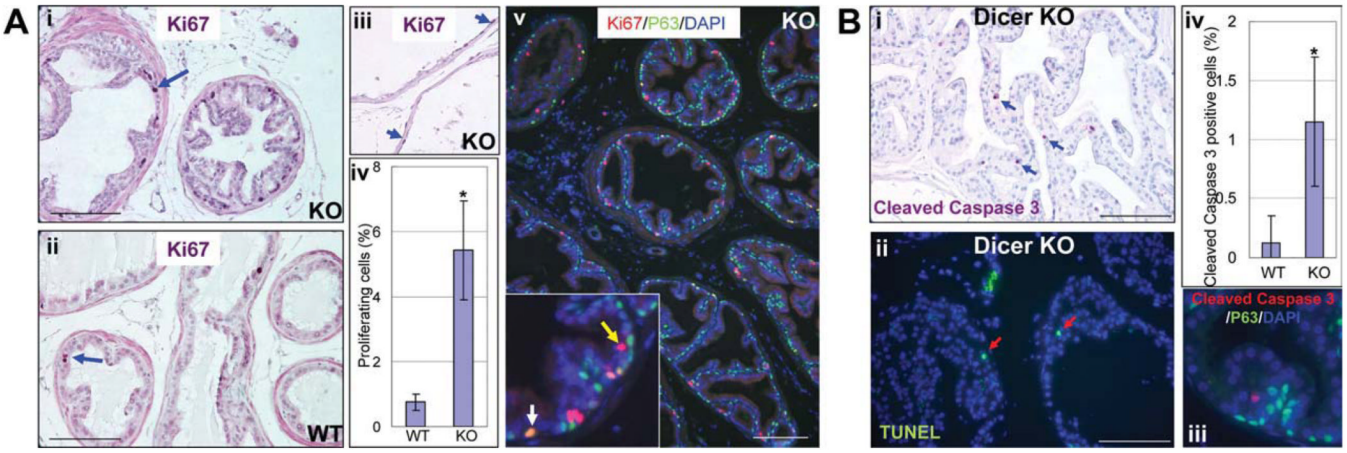

Figure 6.

Increased proliferation and apoptosis in Dicer cKO mouse prostates. **(A):** IHC analysis of Ki67 expression in *Dicer* cKO (i) and WT (ii) mouse prostates. (iii) Ki67 expression in atrophic prostate epithelia in the *Dicer* cKO mice. Bars = 100 μm. (iv) Bar graph compares the proliferating index of WT and cKO mouse prostates. Error bars represent means and STD. *, $p < .0005$. (v) Double staining of Ki67 and P63. Yellow and white arrows point to $Ki67^{+}P63^{-}$ and $Ki67^{+}P63^{+}$ cells, respectively. Bars = 100 μm. **(B):** IHC analysis of cellular apoptosis. (i,ii) Analysis of activity of cleaved caspase three and terminal d-UTP end-labeling (TUNEL). Blue and red arrows point to cells positive for cleaved caspase three and TUNEL staining, respectively. Bars = 100 μm. (iii) Bar graph shows the apoptotic index in WT and *Dicer* cKO mouse prostates. Error bars represent means and STD. *, $p < .0005$. (iv) Double staining of cleaved caspased three and P63.

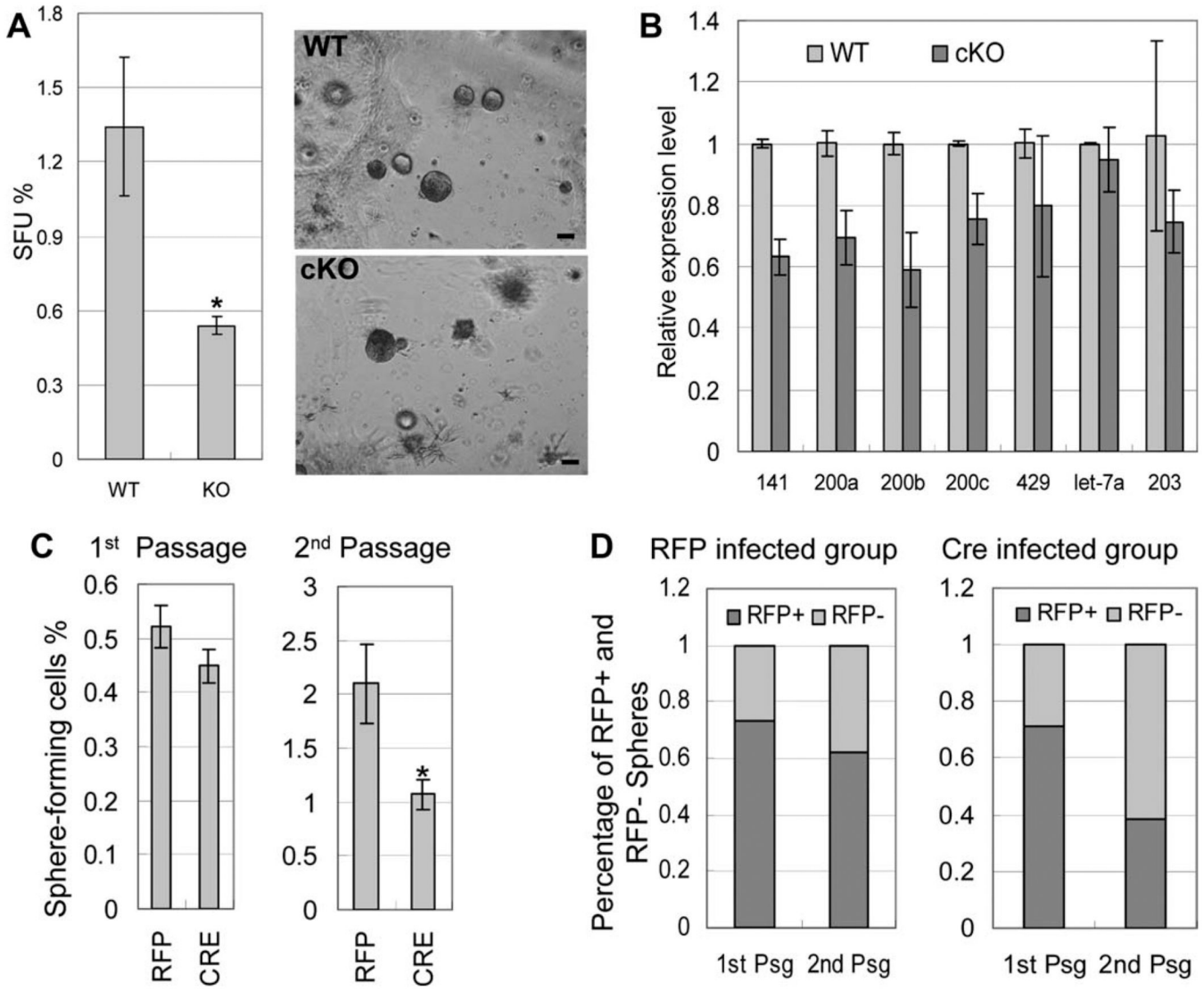

Figure 7.

Dicer ablation impairs the capacity of prostate stem cells to form prostate spheres in vitro. **(A):** Images of prostate spheres and bar graph comparing SFU of WT and Dicer cKO prostate cells. Results were from three independent experiments using three different mice for each group. Bars = 100 μm. Error bars represent means and STD. *p < 5e-08. **(B):** A representative Taqman miRNA assay measuring microRNA expression in WT and *Dicer* cKO prostate sphere cultures. SnoRNA234 was used as an internal control. Data were from two independent experiments using different mice. Error bars represent means and STD. **(C):** Bar graphs comparing SFU of *Dicer*$^{fl/fl}$ cells infected with the Cre lentivirus and the control RFP lentivirus in prostate sphere cultures of the first and second generations. Error bars represent means and STD from triplicate experiments. *p < .05. **(D):** Bar graph comparing the percentage of red spheres in the first and second generations of prostate sphere cultures using *Dicer*$^{fl/fl}$ cells infected with the Cre lentivirus and the control RFP lentivirus. Abbreviations: RFP, red fluorescent protein; SFU, sphere forming unit.